Statistical Determination of Bulk Flow Motions

[1]Yong-Seon Song, [1,2]Cristiano G. Sabiu, [1]Robert C. Nichol and [2]Christopher J. Miller*
[1]*Institute of Cosmology & Gravitation, University of Portsmouth, Portsmouth, PO1 3FX, UK*
[2]*Department of Physics & Astronomy, University College London, Gower Street, London, U.K*
[3]*Cerro-Tololo Inter-American Observatory, National Optical Astronomy Observatory, 950 North Cherry Ave., Tucson, AZ 85719, USA*

(Dated: January 7, 2010)

We present here a new parameterization for the bulk motions of galaxies and clusters (in the linear regime) that can be measured statistically from the shape and amplitude of the two–dimensional two–point correlation function. We further propose the one–dimensional velocity dispersion (v_p) of the bulk flow as a complementary measure of redshift–space distortions, which is model–independent and not dependent on the normalisation method. As a demonstration, we have applied our new methodology to the C4 cluster catalogue constructed from Data Release Three (DR3) of the Sloan Digital Sky Survey. We find $v_p = 270^{+433}$ km/s (also consistent with $v_p = 0$) for this cluster sample (at $\bar{z} = 0.1$), which is in agreement with that predicted for a WMAP5–normalised ΛCDM model (i.e., $v_p(\Lambda\mathrm{CDM}) = 203\,\mathrm{km/s}$). This measurement does not lend support to recent claims of excessive bulk motions ($\simeq$ 1000 km/s) which appear in conflict with ΛCDM, although our large statistical error cannot rule them out. From the measured coherent evolution of v_p, we develop a technique to re-construct the perturbed potential, as well as estimating the unbiased matter density fluctuations and scale–independent bias.

PACS numbers: draft

I. INTRODUCTION

A decade ago, astronomers discovered the expansion of the Universe was accelerating via the cosmological dimming of distant supernovae [1, 2]. Since then, the combination of numerous, and diverse, experiments has helped to establish the Cosmological Constant (specifically a ΛCDM model) as the leading candidate to explain this cosmic acceleration. However, with no theoretical motivation to explain the required low energy vacuum of the ΛCDM model, there is no reason to preclude alternative models, especially those based upon the possible violation of fundamental physics which have yet to be proven on cosmological scales [3, 4].

In addition to using geometrical probes like Supernovae to constrain the cosmic acceleration, tests based on the formation of structures in the Universe also provide a method for validating our cosmological models. In particular, we can investigate the consistency between the geometrical expansion history of the Universe and the evolution of local density inhomogeneities to help reveal a deeper understanding of the nature of the cosmic acceleration [5–9].

In general, there are three observables that can be used to quantify structure formation in the Universe, namely geometrical perturbations, energy–momentum fluctuations and peculiar velocities, all of which will be measured to high precision via future experiments like DES, LSST, JDEM and Euclid (see details of these experiments in the recent FoMSWG report [10]). In more detail, such weak lensing experiments measure the integrated geometrical effect on light as its trajectory is bent by the gravitational potential. Likewise, galaxies (and clusters of galaxies) measure the correlations amongst large–scale local inhomogeneities, while the observed distortions in these correlations (in redshift–space) can be used to extract information about peculiar velocities [11–14]. In this paper, we explore the cosmological constraints on the physics of cosmic acceleration using peculiar velocities, as it is one of the key quantities required for a consistency test of General Relativity [15, 16].

Early observational studies of the peculiar velocity field, or "bulk flows", have produced for many years discrepant results [17], primarily due to small sample sizes and the heterogeneous selection of galaxies. However, a recent re-analysis of these earlier surveys [18] has now provided a consistent observational picture from these data and finds significant evidence for a larger than expected bulk motion. This is consistent with new measurements of the bulk motion of clusters of galaxies using a completely different methodology[19, 20], which leads to the intriguing situation that all these measurements appear to be significantly greater in amplitude, and scale, than expected in a concordance, WMAP5–normalised ΛCDM cosmological model. Such discrepancies with ΛCDM may give support to exotic cosmological models like modified gravity [21].

Given the importance of these large–scale bulk flow measurements, we propose here an alternative methodology to help check these recent claims of anomalously high peculiar velocities which are inconsistent with the standard ΛCDM cosmology. We start by outlining a statistical determination of bulk flow motions using redshift–space distortions in large-scale galaxy or cluster surveys. Such redshift-space distortions are easily seen in the two–dimensional correlation function ($\xi_s(\sigma, \pi)$), which is the

*Electronic address: yong-seon.song@port.ac.uk

decomposition of the correlation function into two vectors; one parallel (π) to the line–of–sight and the other perpendicular (σ) to the line–of–sight. On small scales, any incoherent velocities of galaxies within a single dark matter halo (or cluster) will just add to the cosmological Hubble flow thus causing the famous "Fingers-of-God" (FoG) effect which stretches the 2-D correlation function preferentially in line-of-sight (π) direction. These distortions depend on the inner dynamics and structure of halos and therefore, any cosmological information is difficult to distinguish from the halo properties. However, on large scales (outside individual dark matter halos), the peculiar velocities become coherent and follow the linear motion of the matter thus providing crucial information on the formation of large-scale structure [22].

In this paper, we compare predictions for $\xi_s(\pi,\sigma)$ to observations based on the C4 cluster catalogue [23] from the Sloan Digital Sky Survey (SDSS) [24]. Using the Kaiser formulation [22], a theoretical model for $\xi_s(\pi,\sigma)$ is fit to the measured 2-D correlation function in configuration–space, with the ξ_s parameterised by a shape dependent part and a coherent evolution component. We also propose that the 1-D linear velocity dispersion (v_p) is a interesting quantity to report when measuring redshift–space distortions, and complementary to traditional quantities like β, f or $f\sigma_8$ discussed recently [11–13], as it is independent of both bias and the normalisation method. Therefore, the measured v_p provides an unbiased tracer of the evolution of structure formation.

II. STATISTICAL DETERMINATION OF PECULIAR VELOCITY

The redshift–space two-point correlation function of mass tracers ($\xi_s(\sigma,\pi)$) is an anisotropic function [22]. On small scales, it is elongated in the π-direction by the "Fingers-of-God" effect, while on large scales, the gravitational infall into overdense regions preferentially compresses the correlation function in the σ direction. Therefore, peculiar velocities can be statistically measured by analyzing the observed anisotropic pattern of $\xi_s(\sigma,\pi)$ in both the linear and non-linear regimes.

$\xi_s(\sigma,\pi)$ is derived from the convolution of $\xi(r)$ with a probability distribution function of peculiar velocities along the line of sight, which is usually called the streaming model [25]. Even with the simplest form of a Gaussian probability distribution, the streaming model describes the suppression effect on $\xi_s(\sigma,\pi)$ on small scales.

In the linear regime, the density fluctuations and peculiar velocity are coherently evolved through the continuity equation, which is known as the Kaiser limit. Thus the known correlation function of $\xi(r)$ from the linear perturbation theory developed by gravitational instability is uniquely transformed into $\xi_s(\sigma,\pi)$ [26–30].

The large scale limit of the streaming model is consistent with the Kaiser limit [22], when both the density and peculiar velocity fields are treated as statistical quantities [31]. This consistency test was developed further to show that, even in the Kaiser limit, the description of $\xi_s(\sigma,\pi)$ in linear theory can be modified due to the correlation between the "squashing" (in the σ direction) and dispersion effects (in the π direction) [32]. With the assumption of a Gaussian pair-wise velocity distribution function, the dispersion effect smears into the Kaiser limit description of $\xi_s(\sigma,\pi)$ at around the percent level which for our present work can be ignored. Thus we adopt the Kaiser limit for the description of $\xi_s(\sigma,\pi)$ in linear regime while considering dispersion effect as a systematic uncertainty. We introduce below a new parameterisation of $\xi_s(\sigma,\pi)$ in terms of the cosmological parameters and construct a method to measure the mean velocity dispersion v_p in a model independent way.

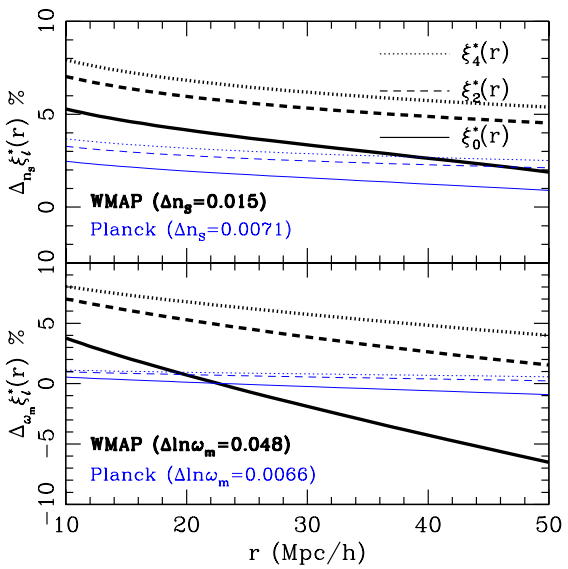

FIG. 1: $\Delta\xi_l^*(r)$ for various CMB experiments priors. In the upper panel, we show the change in $\xi_l^*(r)$ for variations in ω_m. In the lower panel, we show the change in $\xi_l^*(r)$ as a function of n_S. The thick black curves are based on WMAP priors, while the thin blue curves are for Planck prior. On the y-axis, we focus on the range of scales probed by recent and planned reshift–space distortion measurements.

A. Model independent parameterisation of power spectra

The discovery of cosmic acceleration has prompted rapid progress in theoretical cosmological research and prompted many authors to propose modification to the law of gravity beyond our solar system. For example, some theories based upon General Relativity can be modified by screening (or anti-screening) the mass of gravitationally bound objects [3], while others include a non-trivial dark energy component (e.g. interacting dark energy [33, 34], or clumping dark energy [35]) thus breaking the dynamical relations between density fluctuations

and peculiar velocity in the simplest dark energy models. These theoretical ideas motivate us to express various power spectra of the density field in a more convenient way to test such theories.

We assume a standard cosmology model for epochs earlier than the last scattering surface, and that the coherent evolution of structure formation from the last scattering surface to the present day is undetermined due to new physics relevant to the cosmic acceleration. Thus we divide the history of structure formation into two regimes; epochs before matter-radiation equality (a_{eq}) and a later epoch of coherent evolution of unknown effect on structure formation from new physics.We can then express various power spectra of the density field splits into these two epochs, with the shape-dependent part determined by knowledge of our standard cosmology, and the coherent evolution part only affected by new physics. Mathematically, this is written as,

$$\begin{aligned} P_{\Phi\Phi}(k,a) &= D_\Phi(k) g_\Phi^2(a), \\ P_{bb}(k,a) &= D_m(k) g_b^2(a), \\ P_{\Theta_m\Theta_m}(k,a) &= D_m(k) g_{\Theta_m}^2(a)\,, \end{aligned} \tag{1}$$

where Φ denotes the curvature perturbation in the Newtonian gauge,

$$ds^2 = -(1+2\Psi)dt^2 + a^2(1+2\Phi)dx^2\,, \tag{2}$$

and Θ_m denotes the map of the re-scaled divergence of peculiar velocity θ_m as $\Theta_m = \theta_m/aH$. These power spectra are then partitioned into a scale–dependent part ($D_\Phi(k), D_m(k)$) and a scale-independent (coherent evolution) component (g_Φ, g_b, g_{Θ_m}). We define here $g_b = b\, g_{\delta_m}$ where b is the standard linear bias parameter between galaxy (or cluster) tracers and the underlying dark matter density.

The shape of the power spectra is determined before the epoch of matter–radiation equality. Under the paradigm of inflationary theory, initial fluctuations are stretched outside the horizon at different epochs which generates the tilt in the power spectrum. The predicted initial tilting is parameterised as a spectral index (n_S) which is just the shape dependence due to the initial condition. When the initial fluctuations reach the coherent evolution epoch after matter-radiation equality, they experience a scale-dependent shift from the moment they re-enter the horizon to the equality epoch. Gravitational instability is governed by the interplay between radiative pressure resistance and gravitational infall. The different duration of modes during this period results in a secondary shape dependence on the power spectrum. This shape dependence is determined by the ratio between matter and radiation energy densities and sets the location of the matter-radiation equality in the time coordinate. As the radiation energy density is precisely measured by the CMB blackbody spectrum, these secondary shape dependences are parameterised by the matter energy density $\omega_m = \Omega_m h^2$. Both of these parameters are now well–determined by CMB experiments.

The shape factor of the perturbed metric power spectra $D_\Phi(k)$ is defined as

$$D_\Phi(k) = \frac{2\pi^2}{k^3}\frac{9}{25}\Delta^2_{\zeta_0}(k) T^2_\Phi(k) \tag{3}$$

which is a dimensionless metric power spectra at a_{eq}, where $\Delta^2_{\zeta_0}(k)$ is the initial fluctuations in the comoving gauge and $T_\Phi(k)$ is transfer function normalized at $T_\Phi(k\to 0) = 1$. The primordial shape $\Delta^2_{\zeta_0}(k)$ depends on n_S, as $\Delta^2_{\zeta_0}(k) = A_S^2 (k/k_p)^{n_S-1}$, where A_S^2 is the amplitude of the initial comoving fluctuations at the pivot scale, $k_p = 0.002\mathrm{Mpc}^{-1}$. The intermediate shape factor $T_\Phi(k)$ depends on ω_m. The shape factor for matter fluctuations and peculiar velocities $D_m(k)$ are given by the conversion from $D_\Phi(k)$ of,

$$D_m(k) \equiv \frac{4}{9}\frac{k^4}{H_*^4\omega_m^2} D_\Phi(k), \tag{4}$$

where $H_* = 1/2997\,\mathrm{Mpc}^{-1}$.

Unlike the shape part, the coherent evolution component, g_Φ, g_b and g_{Θ_m} are not generally parameterized by known standard cosmological parameters. We thus normalize these growth factors at a_{eq} such that,

$$\begin{aligned} g_\Phi(a_{eq}) &= 1, \\ g_{\delta_m}(a_{eq}) &= a_{eq} g_\Phi(a_{eq}), \\ g_{\Theta_m}(a_{eq}) &= -\frac{d g_{\delta_m}(a_{eq})}{d\ln a}\,. \end{aligned} \tag{5}$$

Instead of determining growth factors using cosmological parameters, we measure these directly in a model-independent way at the given redshift without referencing to any specific cosmic acceleration model and with the minimal assumption of coherent evolution of modes after a_{eq}. Considering the uncertainty in the determination of A_S^2 from the CMB anisotropy, which is degenerate with the optical depth of re-ionization, we combine both A_S^2 and g_X (where X denotes each component of Φ, b and Θ_m) with proper scaling for convenience as $g^*_X = g_X A_S/A^*_S$. Throughout this paper, we use $A^{*2}_S = 2.41\times 10^{-9}$ for the mean A_S^2 value from the WMAP5 results. Our result on measuring the bulk flow motion is independent of our choice of an arbitrary constant A^{*2}_S.

B. Correlation function in the configuration space

In the linear regime of the standard gravitational instability theory, the Kaiser effect (the observed squeezing of $\xi_s(\sigma,\pi)$ due to coherent infall around large–scale structures) can be written in configuration space as,

$$\begin{aligned} \xi_s(\sigma,\pi)(a) &= \left(g_b^{*\,2} + \frac{1}{3}g_b^* g^*_{\Theta_m} + \frac{1}{5}g^{*\,2}_{\Theta_m}\right)\xi_0^*(r)\mathcal{P}_0(\mu) \\ &- \left(\frac{4}{3}g_b^* g^*_{\Theta_m} + \frac{4}{7}g^{*\,2}_{\Theta_m}\right)\xi_2^*(r)\mathcal{P}_2(\mu) \\ &+ \frac{8}{35}g^{*\,2}_{\Theta_m}\xi_4^*(r)\mathcal{P}_4(\mu), \end{aligned} \tag{6}$$

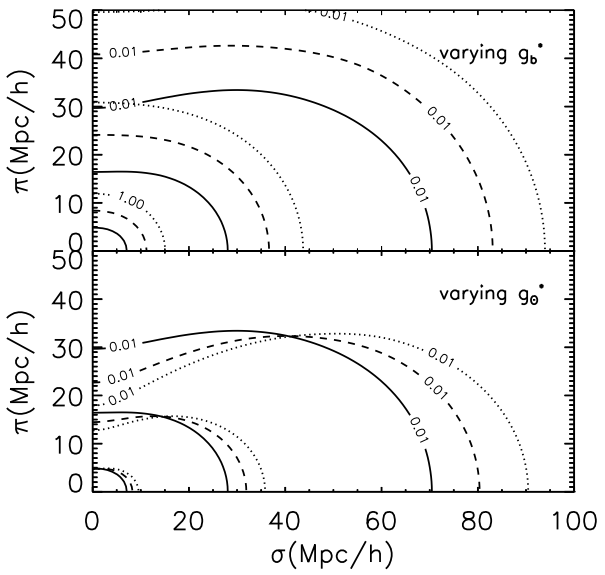

FIG. 2: The $\xi_s(\sigma,\pi)$ correlation function. We plot for three contours of $\xi_s(\sigma,\pi) = 1, 0.1, 0.01$ (from the inner to outer contour). In the upper panel, the solid curves are for a ΛCDM cosmology, while the dash and dotted curves are for models with $g_b = 1.5$ and 2 respectively. In the lower panel, the solid curves are for a ΛCDM cosmology, while the dash and dotted curves are for models with $g_{\Theta_m} = 1.5$ and 2 respectively.

where $\mathcal{P}_l(\mu)$ is the Legendre polynomial and the spherical harmonic moment $\xi_l^*(r)$ is given by,

$$\xi_l^*(r) = \int \frac{k^2 dk}{2\pi^2} D_m^*(k) j_l(kr), \tag{7}$$

where j_l is a spherical Bessel function and $*$ denotes scaling of the shape factor with A_S^{*2}.

As discussed above, we ignore the effect on $\xi_s(\sigma,\pi)$ of the small-scale velocity dispersions within a single dark matter halo [32] as the effect is only a few percent, and split Eqn. 6 into a shape–dependent part ($\xi_l^*(r)$), which is determined by the cosmological parameters (n_S and ω_m), and a coherent evolution component, which is parameterised by $g_{b\,i}^*$, $g_{\Theta_m\,i}^*$ at the targeted redshift z_i. The shape part is therefore almost completely determined by CMB priors, while the coherent evolution of structure formation can be determined from fitting $\xi_s(\sigma,\pi)$, in redshift–space, as a function of redshift.

In Figure 1, we present the effect of CMB priors on the value of $\xi_l^*(r)$. In the top panel of Fig. 1, we provide the expected variation in $\xi_l^*(r)$ from varying ω_m. We see that varying a_{eq} causes greater tilting in the shape of $\xi_l^*(r)$, since larger scale modes can come into the horizon earlier. In addition to this contribution, the overall amplitude of $\xi_l^*(r)$ depends on ω_m by a weighted transformation between $D_\Phi(k)$ and $D_m(k)$. Considering the marginalisation over CMB priors, we expect a discrepancy of $\simeq 5\%$ with WMAP5 measurements, and just a few percent effect with the projected Planck priors.

In the bottom panel of Fig. 1, the dependence of $\xi_l^*(r)$ on n_S is given for both WMAP5 and Planck priors. The overall shifting can be re-scaled by adjusting the pivot point to the effective median scale of the survey. With the measured WMAP5 prior of $\Delta n_S = 0.015$ [36], we expect variations of a few percent on the shape, while for an estimated Planck prior of $\Delta n_S = 0.0071$ [37], we expect $\xi_l^*(r)$ to be nearly invariant to n_S. The shape of $\xi_l^*(r)$ is affected maximally during the intermediate epoch, from horizon crossing to the matter-radiation epoch. The decay rate of the inhomogeneities differs by the ratio between matter and radiation energy densities.

Once CMB constraints are placed on the shape part of Eqn. 6, the coherent history of structure formation is obtained from the anisotropic moment of $\xi_s(\sigma,\pi)$. Even though both $g_{b\,i}^*$ and $g_{\Theta_m\,i}^*$ weight the evolution sector simultaneously, their contribution to $\xi_s(\sigma,\pi)$ are different, which enables us to discriminate $g_{\Theta_m\,i}^*$ from $g_{b\,i}^*$. In the monopole moment, $g_{b\,i}^*$ is the dominant component since $g_{b\,i}^* > g_{\Theta_m\,i}^*$ unless their is an excessive bulk flow. Thus the variation of $g_{b\,i}^*$ generates a near isotropic amplification as illustrated in the top panel of Figure 2. In the quadrupole moment, the cross-correlation between δ_m and Θ_m is leading order. The reversed sign of the quadrupole moment results in the squashing effect, and it is sensitive to the variation of $g_{\Theta_m\,i}^*$ as the cross-correlation is the leading order. In the bottom panel of Figure 2 the variation of $g_{\Theta_m\,i}^*$ mainly contributes to the anisotropic moment. It is this signal which allows both $g_{b\,i}^*$ and $g_{\Theta_m\,i}^*$ to be probed separately using the anisotropic structure of $\xi_s(\sigma,\pi)$. The contribution from the term having peculiar velocity autocorrelation is not significant if excessive bulk flows are excluded.

C. Implication for cosmology from measuring $g_{b\,i}^*$ and $g_{\Theta_m\,i}^*$

A measurement of $g_{\Theta_m\,i}^*$ is equivalent to the quantity $f\sigma_8^{\rm mass}$ [14] and therefore, an excellent test of dark energy models (where f is the logarithmic derivative of the linear growth rate and $\sigma_8^{\rm mass}$ is the root-mean-square mass fluctuation in spheres with radius $8h^{-1}$Mpc). While cosmological test of $g_{\Theta_m\,i}^*$ are free from bias, which is notoriously difficult to measure accurately in a model–independent way, the reported value of $g_{\Theta_m\,i}^*$ does depend on the normalization which is also poorly constrained (i.e., primordial amplitude) or model–dependent (i.e., $\sigma_8^{\rm mass}$).

Thus, we introduce a more convenient parameterisation of peculiar velocity which is independent of these normalization issues. The measured $g_{\Theta_m\,i}^*$ (in the redshift bin i) which can be translated into the one-dimensional (1-D) velocity dispersion in that redshift bin (v_p^i) by,

$$v_p^{i\,2} = g_{\Theta_m\,i}^{*2} \frac{H^2}{3} \int_0^\infty \frac{dk}{k} D_m(k) dk. \tag{8}$$

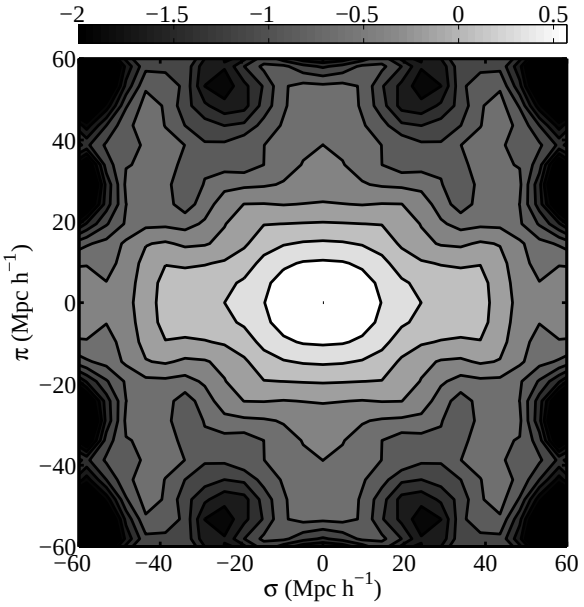

FIG. 3: The 2-D two–point correlation function ($\xi_s(\sigma,\pi)$) for the SDSS DR3 C4 cluster survey with a median redshift of $\bar{z}$=0.1. The contours have been slightly smoothed.

In this formula, there is a degeneracy between $g^*_{b\,i}$ and $g^*_{\Theta_m\,i}$ which cannot be solely broken by fitting $\xi_s(\sigma,\pi)$; instead we simultaneously fit for v_p^i and b^i from the data and then marginalize over the bias to obtain v_p (independent of b) in that redshift bin. Therefore, if our statistical determination of the history of v_p^i can be combined with an independent measurement of bias, then v_p^i can be determined precisely. The scaled parameter $g^*_{\Theta_m\,i}$ depends on all shift factors; the primordial amplitude or the enhancement of D_m due to varying ω_m, as well as later time Θ_m evolution. But the estimation of v_p from $g^*_{\Theta_m\,i}$ is independent of the uncertainty in the overall shifting.

If the evolution of $g^*_{\Theta_m}$ is measured, it can be used to reconstruct other coherent growth factors. The coherent growth factor of Φ can be given using the Euler equation,

$$g^*_\Phi = \frac{2}{3}\frac{aH}{H_*^2\omega_m}\left(g^*_{\theta_m} + \frac{dg^*_{\theta_m}}{d\ln a}\right), \tag{9}$$

where no anisotropy condition is used. If the Poisson equation is validated then the re-constructed g^*_Φ can be used to derive $g^*_{\delta_m}$ using the relation $g^*_{\delta_m} = ag^*_\Phi$. Then this estimated matter fluctuation evolution can be used to determine bias from the measured $g^*_{b\,i}$ as $b = g^*_{b\,i}/g^*_{\delta_m}$.

III. REDSHIFT–SPACE DISTORTIONS FROM CLUSTERS OF GALAXIES

As a demonstration of the parameterization discussed above, we present here a measurement of the redshift–space 2-D two–point correlation function ($\xi_s(\sigma,\pi)$) for clusters of galaxies selected from the SDSS. We use an updated version of the C4 cluster catalogue [23] based on Data Release 3 (DR3; [38]) of the SDSS. Briefly, the C4 catalogue identifies clusters in a seven-dimensional galaxy position and colour space (righ ascension, declination, redshift, $u-g, g-r, r-i, i-z$) using the SDSS Main Galaxy spectroscopic sample. This method greatly reduces the twin problems of projection effects and redshift space distortions in identifying physically–bound galaxy groups. This catalogue is composed of ~ 2000 clusters in the redshift range $0.02 < z < 0.15$.

The estimation of the correlation function relies crucially on our ability to compare the clustering of the data to that of a random field. Thus any artificial structures in the data must be considered when constructing the random catalogue. These problems include incompleteness, such as the angular mask (e.g. survey boundaries, bright stars and dust extinction in our own galaxy), and the radial distribution where at large distances, the mean space density decreases as we approach the magnitude limit of the survey. We have constructed random samples which takes these issues into account, i.e., the angular positions are randomly sampled from a sphere to lie within the DR3 mask, while the redshifts are obtained from a smooth spline fit to the real C4 redshift distribution (which removes true large scale structures). The random samples are then made to be 50 times denser than the real data to avoid Poisson noise.

In Figure 3, we show our estimation of the $\xi_s(\sigma,\pi)$ binned into with 6 configuration–space bins up to 60 Mpc (one bin per 10Mpc). Separations of less than 10 Mpc are removed to reduce the FoG effect. Error on $\xi_s(\sigma,\pi)$ were derived using the jackknife method [39], which involves dividing the survey into N sub-sections with equal area (and thus volume) and then computing the mean and variance of $\xi_s(\sigma,\pi)$ from these N measurements of the correlation function with the i^{th} region removed each time (where $i = 1...N$).

In our analysis, we divided the whole C4 area into $N = 30$ sub-subsections and determine the variance from [40],

$$\sigma^2_\xi(r_i) = \frac{N_{jack}-1}{N_{jack}}\sum_{k=1}^{N_{jack}}[\xi_k(r_i) - \overline{\xi}(r_i)]^2, \tag{10}$$

where N_{jack} is the number of jackknife samples used and r_i represents a single bin in the $\sigma-\pi$ configuration space. Then we compute

$$\overline{\xi}(r_i) = \frac{1}{N_{jack}}\sum_{k=1}^{N_{jack}}\xi_k(r_i), \tag{11}$$

and the normalised covariance matrix is estimated from [39],

$$C_{ij} = \frac{N_{jack}-1}{N_{jack}}\sum_{k=1}^{k=N_{jack}}\Delta_i^k\Delta_j^k, \tag{12}$$

where,

$$\Delta_i^k = \frac{\xi_k(r_i) - \overline{\xi}(r_i)}{\sigma_\xi(r_i)}. \tag{13}$$

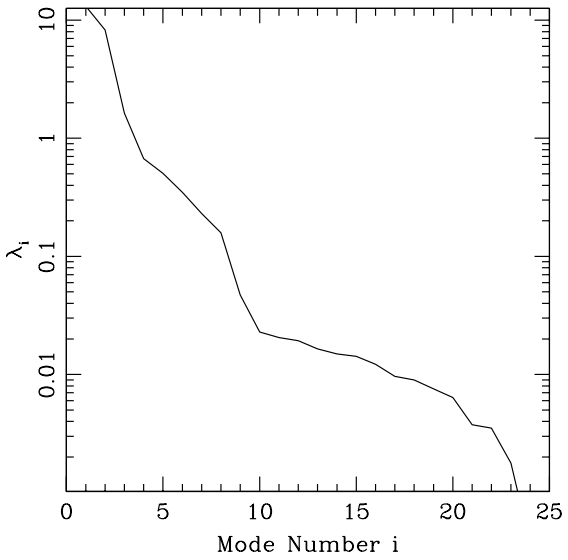

FIG. 4: An ordered list of the Eigenvalues for our cluster covariance matrix.

Before we invert C_{ij} in Eqn. 12, we note that the values of C_{ij} are estimated to limited resolution,

$$\Delta C_{ij} = \sqrt{\frac{2}{N_{jk}}} \tag{14}$$

and therefore, if N_{jk} is small, or there are degeneracies within C_{ij}, the inversion will be affected. This problem can be eliminated by performing a Single Value Decomposition (SVD) of the matrix,

$$C_{ij} = U^{\dagger}_{ik} D_{kl} V_{lj}, \tag{15}$$

where U and V are orthogonal matrices that span the range and the null space of C_{ij} and $D_{kl} = \lambda^2 \delta_{kl}$, a diagonal matrix with singular values along the diagonal. In doing the SVD, we select the dominant modes to contribute to the χ^2 by requiring that $\lambda^2 > \sqrt{2/N_{jk}}$.

In Figure 4, we rank the eigenvalues (λ_i) for the increasing eigenmodes and see a "kink" in the distribution which we interpret as indicating a transition in the signal–to–noise of the eigenmodes, i.e., only the first ten modes contain most of the signal, while higher-ordered modes are dominated by noise. We therefore remove eigenmodes beyond this kink (with $\lambda_i < 0.01$) where the eigenvalues start to flatten out.

A. Statistical determination of large scale flow

As discussed in the Introduction, there is recent evidence for excessive bulk flow motions compared to the WMAP5-normalised ΛCDM model [18] and therefore, it is important to confirm these results as it may indicate evidence for an alternative explanation for the observed cosmic acceleration such as modified gravity. In this paper, we provide a first demonstration of our new parameterization using clusters of galaxies from the SDSS. In detail, we attempt to model the "squashing" of the 2-D correlation function of the C4 cluster sample seen in Figure 5 using the formalism presented herein. We do however caution the reader that we expect the limited size of the DR3 sample to leads to large statistical errors, due to a significant shot–noise contribution because of their low number density. However, future cluster and galaxy samples (e.g., LRGs) should provide stronger constraints and provide a more robust test of these high bulk flow measurements in the literature.

In Figure 5, we provide the best fit parameters b and v_p for the C4 correlation function presented in Figure 3 and there is as expected a clear anti-correlation between these two parameters because the anisotropic amplitude is generated by cross-correlations in the density and peculiar velocity fields. The best fit value from Figure 5 is $v_p = 270^{+433}$ km/s (at the 1σ level marginalised with other parameters including b) and is consistent with $v_p = 0$. We do not quote the negative bound of the error on v_p as it is below zero and thus has no physical meaning. Instead, we quote the upper bound on v_p and note that our result is consistent with zero. Our measurement of v_p is close to the predicted value of 203 km/s for a WMAP5–normalised ΛCDM model.

We propose above that v_p is a complementary parameter for reporting such peculiar velocity measurements. The parameter g_Θ, which is equivalent to $f\sigma_8$, is not determined precisely without the prior information of A_S. But when we report our measurement with v_p, there is no uncertainty due to other cosmological parameters which are not determined accurately, as it is equivalent to g^*_Θ determined statistically from redshift space distortion. The observed value v_p at a given redshift is not only independent of bias but also independent of normalisation.

B. Reconstruction of matter density field from v_p

We convert v_p measurement into g_Θ using A_s from WMAP5 (g_Θ: coherent growth factor of peculiar velocity, and it is equivalent to $f\sigma_8$ in other parameterizations). With the evolution of g_Θ known, dynamics of perturbations are reconstructed to provide the history of Ψ through the Euler equation. In most theoretical models, the time variation of v_p is minimal at these low redshifts discussed here for the C4 sample ($z \simeq 0.1$), which allows us to ignore the time-derivative part in Eq. 9. Therefore, it is straightforward to transform the coherent evolution of Θ into the coherent evolution of Ψ. If we assume no anisotropic stress, then it is easy to convert to the coherent evolution of Φ, g_Φ.

We are able to determine matter density fluctuations through the Poisson equation. We calculate the coherent growth of δ_m, $g_\delta = 0.7$, which is related to g_Φ as

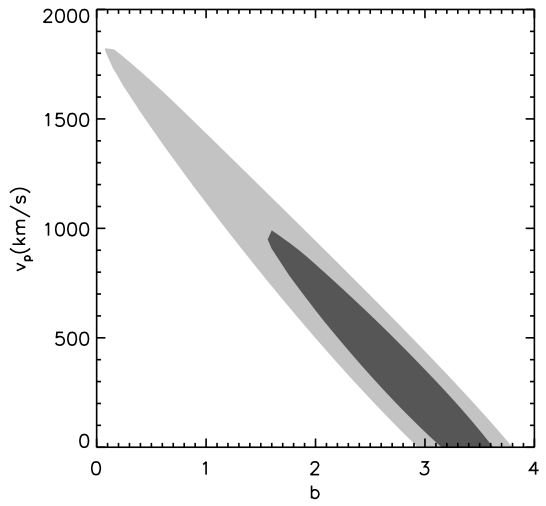

FIG. 5: The 2-D contours between b and v_p with the DR3 cluster sample.

$g_\delta = a g_\Phi$, if no modified Poisson equation is assumed. Finally, the estimated g_δ can be used to derive bias using measured g_b^*. Through fitting to the redshift distortion effect, we extract both g_b^* and g_Θ^*. The density fluctuation evolution g_δ is estimated only from g_Θ^*, and the other measurement g_b^* is not yet used. The combination of the estimated g_δ and the measured g_Θ^* provides bias from $b = g_b^*/g_\delta = 2.9 \pm 0.8$, which is fully consistent with our expectations for such massive clusters of galaxies in the C4 sample.

IV. DISCUSSION

We outline in this paper a new theoretical model for $\xi_s(\pi, \sigma)$, the 2-D two–point correlation function in configuration–space, which allows us to constrain the bulk flow motion of matter on large scales. We also propose that the 1-D linear velocity dispersion (v_p) is a interesting quantity to report when measuring redshift–space distortions. We demonstrate this method using C4 clusters from the SDSS and find a value for v_p that is consistent with a WMAP5–normalised ΛCDM cosmology (within our large statistical errors). Our observed value for these bulk flows is marginally inconsistent with other recent observations in the literature, which find an excess flow compared to a WMAP5–normalised ΛCDM model [18–20]. We do not discuss this further as we plan to revisit these measurements using larger datasets and different tracers of the density field.

As discussed in Section II-C, our measurement of v_p is correlated with g_b, which is the combination of b and δ_m, since the observed anisotropic shape of the 2-D correlation function in redshift–space is generated by a cross correlation between the density field and peculiar velocities. However, one of the important implications of our method is that we can measure v_p without knowing how to decompose g_b, and thus without the uncertainty of determining b.

There are however some caveats to our analysis. We do not analyse our data in Fourier space, but in configuration space. Small scales have been removed from our data analysis (< 10Mpc), to ensure that the FoG effect will not contaminate our results. Our methodology is insensitive to a possible shape dependence at large scales for any exotic reason; scale dependent later time growth (e.g. f(R) gravity models [41]), or scale–dependent bias at large scales. In follow-up studies, we will measure the redshift–space distortions in Fourier space to test the effect of small–scales on our results. In addition, the formulation to derive ξ_s used in this paper can be slightly biased due to the dispersion effect studied in [32]. This effect is not parameterised properly here, but the reported level of uncertainty is approximately 5% which is much smaller than the statistical errors on our present measurements. Therefore, we dismiss this shift here but it is worth revisiting this issue in the future to know how to incorporate this effect in a new parameterisation.

Finally, Song and Percival [13] recently proposed a method to re-construct the structure formation observables from Θ measurements. Although it is not yet estimated precisely in that narrow range of measured values, we apply their methodology in practice. From the observed coherent evolution of Θ at $z = 0.1$ from the DR3 C4 clusters, we re-construct Ψ, Φ and δ_m. We then find that bias can be derived from the estimated δ_m and the measured g_b^*. Here, for the first time, we estimate bias from peculiar velocity measurements only. The estimated values are reasonable at $b = g_b^*/g_\delta = 2.9 \pm 0.8$. It is not precise measurement yet, as the time variation is ignored, but we will revisit this in a following paper.

Acknowledgments

The authors would like to thank Nick Kaiser, Kazuya Koyama and Will Percival for helpful conversations, Prina Patel for useful suggestions on the presentation of this article, and the referee for helpful comments. Y-SS, RCN and CGS are grateful for support from STFC .

[1] S. Perlmutter et al. (Supernova Cosmology Project), Astrophys. J. **517**, 565 (1999), astro-ph/9812133.

[2] A. G. Riess et al. (Supernova Search Team), Astron. J. **116**, 1009 (1998), astro-ph/9805201.

[3] G. Dvali, G. Gabadadze, and M. Porrati, Physics Letters B **485**, 208 (2000), hep-ph/0005016.

[4] S. M. Carroll, A. de Felice, V. Duvvuri, D. A. Easson, M. Trodden, and M. S. Turner, Phys. Rev. D **71**, 063513 (2005), astro-ph/0410031.

[5] Y.-S. Song, Phys. Rev. **D71**, 024026 (2005), astro-ph/0407489.

[6] M. Ishak, A. Upadhye, and D. N. Spergel, ArXiv Astrophysics e-prints (2005), astro-ph/0507184.

[7] L. Knox, Y.-S. Song, and J. A. Tyson, Phys. Rev. D **74**, 023512 (2006).

[8] E. V. Linder, Phys. Rev. D **72**, 043529 (2005), astro-ph/0507263.

[9] B. Jain and P. Zhang, Phys. Rev. **D78**, 063503 (2008), 0709.2375.

[10] A. J. Albrecht et al. (2009), 0901.0721.

[11] Y. Wang, JCAP **0805**, 021 (2008), 0710.3885.

[12] L. Guzzo et al., Nature **451**, 541 (2008), 0802.1944.

[13] Y.-S. Song and W. J. Percival, ArXiv e-prints (2008), 0807.0810.

[14] M. White, Y.-S. Song, and W. J. Percival (2008), 0810.1518.

[15] Y.-S. Song and K. Koyama (2008), 0802.3897.

[16] Y.-S. Song and O. Dore, JCAP **0903**, 025 (2009).

[17] D. Sarkar, H. A. Feldman, and R. Watkins, MNRAS **375**, 691 (2007), arXiv:astro-ph/0607426.

[18] R. Watkins, H. A. Feldman, and M. J. Hudson (2008), 0809.4041.

[19] A. Kashlinsky, F. Atrio-Barandela, D. Kocevski, and H. Ebeling (2008), 0809.3734.

[20] A. Kashlinsky, F. Atrio-Barandela, H. Ebeling, A. Edge, and D. Kocevski (2009), 0910.4958.

[21] N. Afshordi, G. Geshnizjani, and J. Khoury (2008), 0812.2244.

[22] N. Kaiser, Mon. Not. Roy. Astron. Soc. **227**, 1 (1987).

[23] C. J. Miller, R. C. Nichol, D. Reichart, R. H. Wechsler, A. E. Evrard, J. Annis, T. A. McKay, N. A. Bahcall, M. Bernardi, H. Boehringer, et al., AJL **130**, 968 (2005), arXiv:astro-ph/0503713.

[24] D. G. York et al. (SDSS), Astron. J. **120**, 1579 (2000), astro-ph/0006396.

[25] M. Davis and P. J. E. Peebles, Astrophys. J. **267**, 465 (1982).

[26] P. B. Lilje and G. Efstathiou, MNRAS **236**, 851 (1989).

[27] C. McGill, MNRAS **242**, 428 (1990).

[28] O. Lahav, P. B. Lilje, J. R. Primack, and M. J. Rees, MNRAS **251**, 128 (1991).

[29] A. J. S. Hamilton, ApJL **385**, L5 (1992).

[30] K. B. Fisher, C. A. Scharf, and O. Lahav, MNRAS **266**, 219 (1994), arXiv:astro-ph/9309027.

[31] K. B. Fisher, Astrophys. J. **448**, 494 (1995), arXiv:astro-ph/9412081.

[32] R. Scoccimarro, Phys. Rev. **D70**, 083007 (2004), astro-ph/0407214.

[33] L. Amendola, Phys. Rev. **D62**, 043511 (2000), astro-ph/9908023.

[34] K. Koyama, R. Maartens, and Y.-S. Song (2009), 0907.2126.

[35] M. Kunz and D. Sapone, Phys. Rev. Lett. **98**, 121301 (2007), astro-ph/0612452.

[36] E. Komatsu et al. (WMAP), Astrophys. J. Suppl. **180**, 330 (2009), 0803.0547.

[37] M. Kaplinghat, L. Knox, and Y.-S. Song, Phys. Rev. Lett. **91**, 241301 (2003), astro-ph/0303344.

[38] J. K. Adelman-McCarthy, M. A. Agüeros, S. S. Allam, K. S. J. Anderson, S. F. Anderson, J. Annis, N. A. Bahcall, C. A. L. Bailer-Jones, I. K. Baldry, J. C. Barentine, et al., ApJs **172**, 634 (2007), 0707.3380.

[39] R. Scranton, D. Johnston, S. Dodelson, J. A. Frieman, A. Connolly, D. J. Eisenstein, J. E. Gunn, L. Hui, B. Jain, S. Kent, et al., Astrophys. J. **579**, 48 (2002), arXiv:astro-ph/0107416.

[40] R. Lupton, *Statistics in theory and practice* (1993).

[41] Y.-S. Song, W. Hu, and I. Sawicki, Phys. Rev. **D75**, 044004 (2007), astro-ph/0610532.

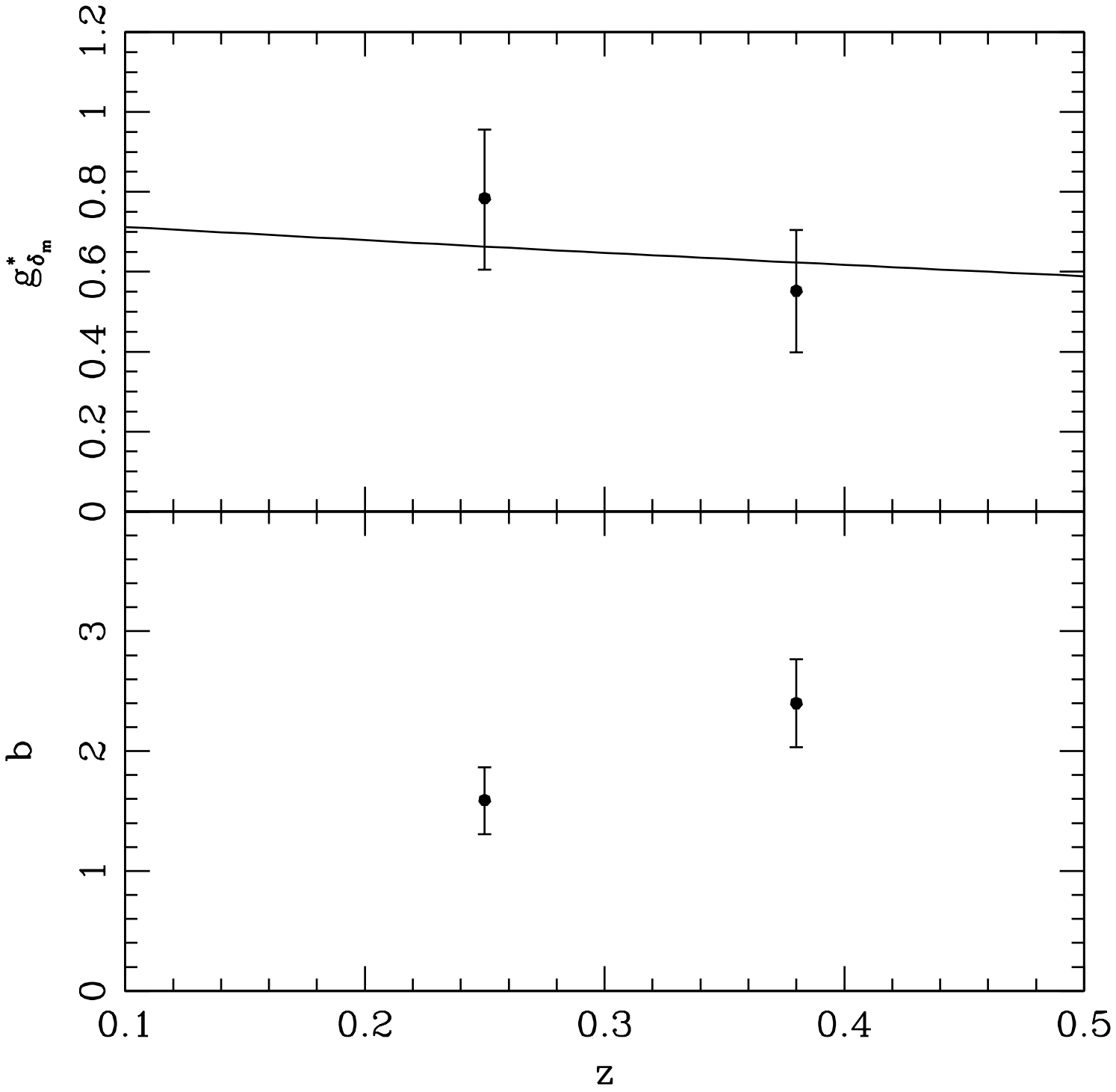
$g^*_{\delta_m}$
0
0.2
0.4
0.6
0.8
1
1.2
b
0
1
2
3
0.1
0.2
0.3
0.4
0.5
z

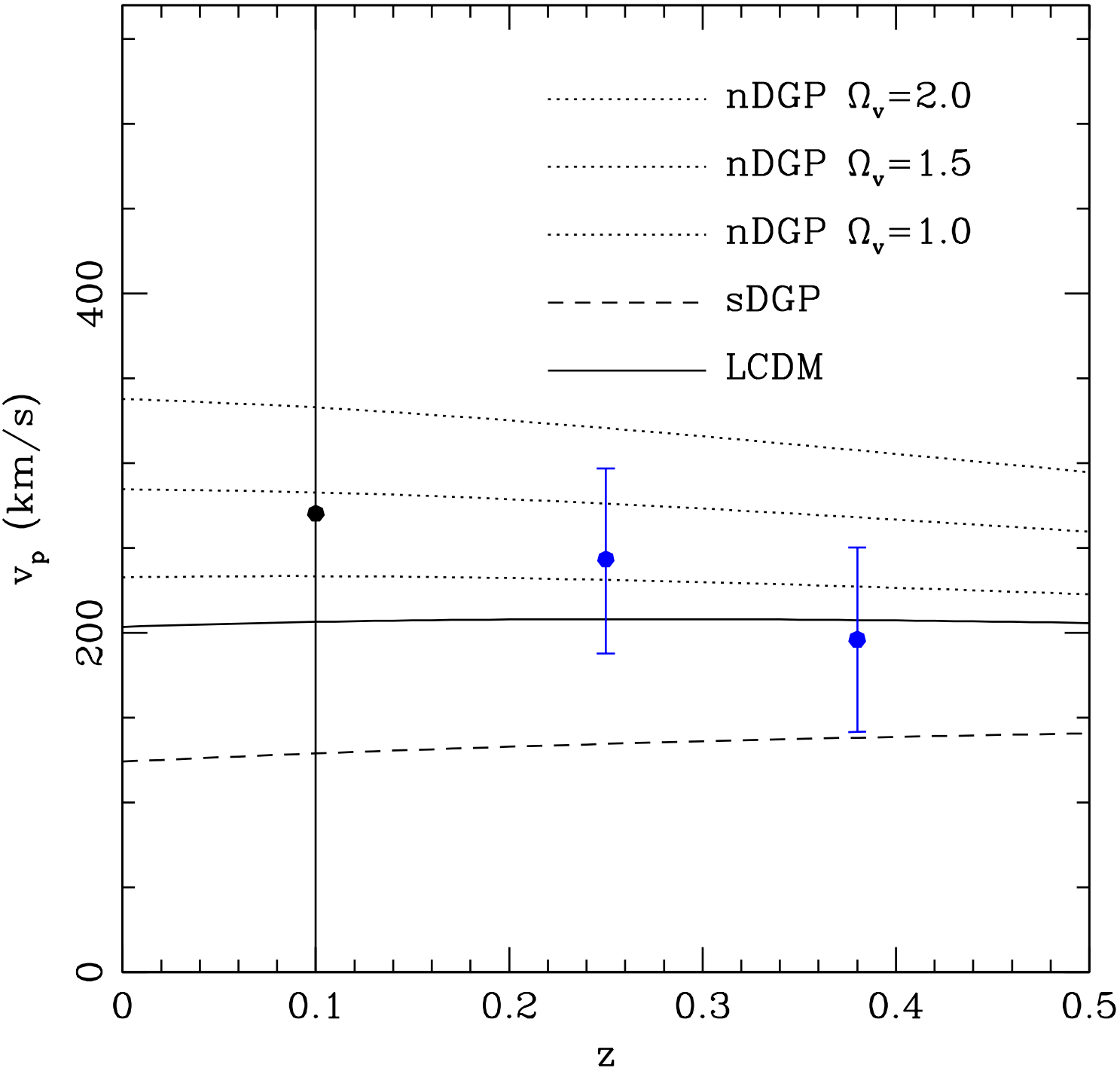
nDGP Ω_v=2.0
nDGP Ω_v=1.5
nDGP Ω_v=1.0
sDGP
LCDM
v_p (km/s)
0
200
400
0
0.1
0.2
0.3
0.4
0.5
z